Electrospray Mass Spectrometry Studies of Poly(Propylene Imine) Dendrimers: Probing Reactivity in the Gas Phase

Jan-Willem Weener, Joost L. J. van Dongen, and E. W. Meijer*

Contribution from the Laboratory of Macromolecular and Organic Chemistry, Eindhoven University of Technology, P.O. Box 513, 5600 MB Eindhoven, The Netherlands

Received December 28, 1998

Abstract: Gas-phase fragmentation patterns of poly(propylene imine) dendrimers DAB-*dendr*-$(NH_2)_n$ with $n = 4$, 8, 16, 32, and 64 are described as a result of MS^n electrospray ionization mass spectrometry (ESI-MS) studies. The generally accepted on-the-average globular shape of dendrimers is supported here by the linear relationship found between the extent of protonation and molecular mass ($M^{2/3}$). Unique fragmentation patterns are observed due to this globular shape. Most fragment ions are readily accounted for when, in addition to nucleophilic displacement reactions, proton shifts and rearrangements are taken into consideration. There is a striking difference in fragmentation behavior between singly charged dendrimers and multiply charged dendrimers. Therefore, it is proposed that the site of protonation within the dendritic framework has a large impact on the fragments observed. The position of the proton is largely dependent on both the relative proton affinities and the Coulomb repulsion between neighboring protonated sites. In case of singly charged dendrimers, electrostatic interactions are absent and the fragmentation is predominantly governed by the relative differences in proton affinity between the basic sites present in the dendrimer. In the gas phase the nitrogen atoms in the core of the dendrimer are the most basic ones present, leading to $[M + H]^+$ ions carrying a protonated diaminobuthane core in all cases. This triggers a cascade of nucleophilic displacement reactions, starting with a bond cleavage of the central dendritic core and finishing with the formation of bis(1,1-propylamine)azetidinium (m/z 172) and fragments derived thereof. In the case of multiply charged dendrimers, Coulomb repulsions lead primarily to protonation of the peripheral tertiary amines, leading to the direct formation of bis(1,1-propylamine)azetidinium. These gas-phase reactions were subsequently utilized as a model for reactions in solution. The gas-phase reactions in ESI-MS thus provided a unique "fingerprint" area of dendrimer fragmentation adducts in the lower m/z range ($m/z < 180$), which matches perfectly with that obtained from dendrimers after prolonged heating in aqueous solution.

Introduction

The synthesis and characterization of well-defined macromolecules, like dendrimers, constitute a relatively new field of great current interest.[1] Dendrimers are prepared in either a convergent[2] or a divergent manner.[3] In the convergent strategy the dendritic wedges are prepared separately and connected to a central core in the final step leading to dendrimers of well-defined architecture next to small amounts of defect dendrimers missing one or more dendritic wedges. The large structural differences between the perfect structure and byproducts make purification relatively facile. Dendrimers prepared by the divergent approach, on the other hand, often suffer from a number of statistical defects, and purification becomes exceedingly difficult with higher generations because the perfect dendrimers differ from the defective ones by only one, or a few, monomer units.[4] Accordingly, powerful analytical methods are required to characterize these highly branched macromolecules in detail.

The analytical techniques that have been applied to characterize dendrimers so far include nuclear magnetic resonance (NMR), size exclusion chromatography (SEC),[5] high-performance liquid chromatography (HPLC),[6] fast-atom bombardment mass spectrometry (FAB-MS),[7] liquid secondary ion mass spectrometry (LSIMS),[8] matrix assisted laser desorption ionization time-of-flight (MALDI-TOF),[9] and more recently electro-

* Author to whom correspondence should be addressed. Phone: 31-40-2473101. Fax: 31-40-2451036. E-mail: E.W.Meijer@tue.nl.

(1) (a) Bosman, A. W.; Janssen, H. M.; Meijer, E. W. *Chem. Rev.* **1999**, *99* (7), 1665−1688. (b) Newkome, G. R.; Moorefield, C. N.; Vögtle, F. *Dendritic Molecules: Concepts, Syntheses and Perspectives*; VCH: Weinheim, Germany, 1996. (c) Frey, H.; Lach, C.; Lorentz, K. *Adv. Mater*. **1998**, *10*, 279−293. (d) Gorman, C. *Adv. Mater*. **1998**, *10*, 295−309.

(2) (a) Fréchet, J. M. J. *Science* **1994**, *263*, 1710. (b) Wooley, K. L.; Hawker, C. J.; Fréchet, J. M. J. *J. Am. Chem. Soc.* **1991**, *113*, 4252. (c) Hawker, C.; Fréchet, J. M. J. *J. Chem. Soc., Chem. Commun*. **1990**, 1010. (d) Wooley, K. L.; Hawker, C. J.; Fréchet, J. M. J. *Angew. Chem*. **1994**, *106*, 123; *Angew. Chem., Int. Ed. Engl*. **1994**, *33*, 82.

(3) (a) Buhleier, E.; Wehner, W.; Vögtle, F. *Synthesis* **1978**, 155. (b) Tomalia, D. A.; Naylor, A. M.; Goddard, W. A. *Angew. Chem., Int. Ed. Engl.* **1990**, *29*, 138. (c) de Brabander van der Berg, E. M. M.; Meijer, E. W. *Angew. Chem.* **1993**, *105*, 1370−1373; *Angew. Chem., Int. Ed. Engl.* **1993**, *32*, 1308−1311. (d) Newkome, G. R.; Yao, Z. Q.; Baker, G. R.; Gupta, V. K. *J. Org. Chem*. **1985**, *50*, 2003.

(4) (a) Tomalia, D. A.; Hedstrand, D. M.; Wilson, L. R. In *Encyclopedia of Polymer Science and Engeneering*, 2nd ed.; Wiley: New York, 1985, Vol. 1, pp 46−92. (b) Newkome, G. R.; Moorefield, C. N.; Baker, G. R.; Johnson, A. L.; Behera, R. K. *J. Org. Chem*. **1992**, *57*, 358. (c) Worner, C.; Mulhaupt, R. *Angew. Chem*. **1993**, *105*, 1367; *Angew. Chem., Int. Ed. Engl.* **1993**, *32*, 1306.

(5) Malenfant, P. R. L.; Groenendaal, L.; Fréchet, J. M. J. *J. Am. Chem. Soc.* **1998**, *120*, 10990−10991.

(6) Bernhard, H. B.; Jaworek, W.; Vögtle, F. *Angew. Chem*. **1992**, *104*, 1609. Van der Wal, Sj.; Mengerink, Y.; Brackman, J. C.; de Brabander, E. M. M.; Jeronimus-Stratingh, C. M.; Bruins, A. P. *J. Chromatogr. A* **1998**, *825*, 135−147.

(7) (a) Moors, R.; Vögtle, F. *Chem. Ber*. **1993**, *126*, 2133. (b) Twyman, L. J.; Beezer, A. E.; Mitchell, J. C. *J. Chem. Soc., Perkin Trans. 1* **1994**, *4*, 407−411.

10.1021/ja984432+ CCC: $18.00
Published on Web 10/22/1999

spray ionization mass spectrometry (ESI-MS).[10] Although the development of ESI-MS is still ongoing and the mechanism of ion formation has not yet been revealed completely,[11] this technique is becoming an increasingly important and efficient tool to investigate macromolecules.[12] The significant advantages offered by ESI-MS include its high sensitivity, "soft" ionization, and the generation of multiply charged ions allowing not only for structural information to be obtained but also for broad molecular weight ranges to be measured.[13] These particular advantages of ESI-MS have led to a breakthrough in the mass spectrometry of large biomolecules.[14] This technique allows for the determination of molecular weights greater than 100 kD. Moreover, the soft method of ionization has proven to be useful in the characterization of organo-metal complexes[15] including metallodendrimers.[16]

MS/MS using collision-activated dissociation (CAD)[17] allows for peptide sequencing and thus makes it possible to elucidate the primary structure of peptides.[18] The site of protonation within the molecule has a large impact on the fragmentation reactions observed. In case of peptides, there is considerable evidence that the site of proton attachment influences the fragmentation reactions, and hence, the structural information obtained.[19] Because the site of proton attachment depends in part on the relative proton affinities of the different basic sites, there is a great interest in gas-phase proton affinities from a biochemical point of view. There are several proton affinity scales, with the most comprehensive one from Lias, Liebmann, and Levin (LLL).[20] All proton affinity ladders show a considerable increase in basicity on going from primary to tertiary amines due to electronic factors.

Scheme 1. Synthesis of Poly(propylene imine) Dendrimers DAB-*dendr*-$(NH_2)_n$ $n = 4, 8, 16, 32, 64$[a]

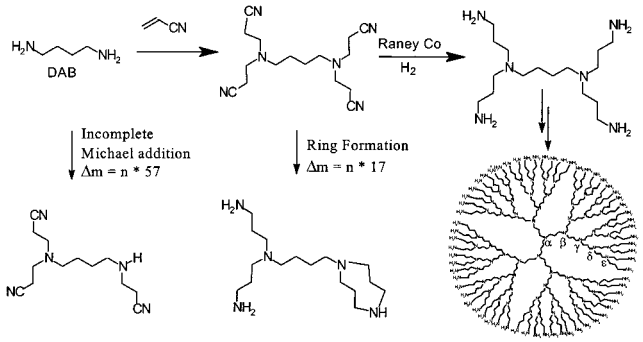

[a] The greek symbols refer to the different shells of tertiary nitrogens. Divergent growth defects caused by incomplete michael addition reactions or ring formations are indicated.

Recently, we presented a detailed ESI-MS analysis on poly(propylene imine) dendrimers showing that all the statistical defects resulting from the divergent growth strategy can readily be assigned.[21] The poly(propylene imine) dendrimers are synthesized starting from diaminobuthane (DAB), the core molecule. Reaction with acrylonitrile in a Michael addition, followed by hydrogenation (H_2/Raney/Co), yields the first generation amine-terminated dendrimer DAB-*dendr*-$(NH_2)_4$. Repetition of this process yields poly(propylene imine) dendrimers containing 4, 8, 16, 32, 64, or 128 nitrile or amine end groups (Scheme 1).[3c]

Simulated mass spectra for all generations were obtained by calculating the probability factors of side reactions (incomplete Michael additions and ring formation during hydrogenation, as indicated in Scheme 1) in the synthesis of the successive generations of dendrimers from the measured ESI-MS spectra.

The protonation behavior of poly(propylene imine) dendrimers has only been described and explained in aqueous solution, using the Ising model.[22] By using natural abundance ^{15}N NMR, we have monitored the chemical shift change of all nitrogen atoms in each shell separately upon change in the pH.[23] From these studies we have learned that, in an *aqueous* environment, the outermost primary amines protonate first followed eventually by the central core atoms, while subsequent protonation is fully controlled by Coulomb forces. The reverse order of basicity in the *gas phase* (and in many organic solvents) is due to the more effective hydration of less highly substituted ammonium ions in an aqueous environment.[24]

In this paper, we describe and discuss the fragmentation patterns observed for both singly and multiply charged dendritic

(8) Lau, R. L. C.; Chan, T. W. D.; Chow, H. F. *Eur. Mass Spectrom.* **1995**, *1*, 371−380.

(9) (a) Leon, J. W.; Fréchet, J. M. J. *Polym. Bull.* (Berlin) **1995**, *35*, 449−455. (b) Derrik, P. J.; Haddleton, D. M.; Lloyd, P. M.; Sahota, H.; Taylor, P. C.; Yeates, S. G. *Polym. Prepr. (Am. Chem. Soc. Div. Polym. Chem.*) **1994**, *35*, 826−827. (c) Walker, K. L.; Kahr, M. S.; Wilkens, C. L.; Xu, Z.; Moore, J. S. *J. Am. Chem. Soc. Mass Spectrom.* **1994**, *5*, 731−739. (d) Kawaguchi, T.; Walker, K. L.; Wilkens, C. L.; Moore, J. S. *J. Am. Chem. Soc.* **1995**, *117*, 2159−2165. (e) Sahota, H.; Lloyd, P. M.; Yeates, S. G.; Derrik, P. J.; Taylor, P. C.; Haddleton, D. M. *J. Chem. Soc., Chem. Commun.* **1994**, *21*, 2445−2446. (f) Ashton, P. R.; Boyd, S. E.; Brown, C. L.; Jayaraman, N.; Nepogodiev, S. A.; Stoddart, J. F. *Chem. Eur. J.* **1996**, *2*, 1115. (g) Wu, Z.; Biemann, K. *Int. J. Mass Spectrom. Ion Processes* **1997**, *165/166*, 349−361.

(10) (a) Stöckigt, D.; Lohmer, G.; Belder, D. *Rapid Commun. Mass Spectrom.* **1996**, *10*, 521−526. (b) Moucheron, C.; Kirch‗De Mesmaker, A.; Dupont-Gervais, A.; Leize, E.; van Dorsselaar, A. *J. Am. Chem. Soc.* **1996**, *118*, 12834−12835. (c) Kallos, G. J.; Lewis, S.; Zhou, J.; Hedstrand, D. M.; Tomalia, D. A. *Rapid Commun. Mass Spectrom.* **1991**, *5*, 383−386. (d) Dvornic, P. R.; Tomalia, D. A. *Macromol. Symp.* **1995**, *98*, 403−428. (e) Pesak, D. J.; Moore, J. F. *Macromolecules* **1997**, *30*, 6467−6482.

(11) (a) Fenn, J. B.; Rosell, J.; Meng, C. K. *J. Am. Soc. Mass Spectrom.* **1997**, *8*, 1147−1157. (b) Fenn, J. B. *J. Am. Soc. Mass Spectrom.* **1993**, *4*, 524−535. (c) Kebarle, P.; Tang, L. *Anal. Chem.* **1993**, *65* (23), 972−986.

(12) Saf, R.; Mirtl, C.; Hummel, K. *Acta Polym.* **1997**, *48*, 513−526.

(13) Przybylski, M.; Glocker, M. O. *Angew. Chem., Int. Ed. Engl.* **1996**, *35*, 806−826.

(14) (a) Fenn, J. B.; Mann, M.; Meng, C. K.; Wong, S. F.; Whitehouse, C. M. *Science* **1989**, *246*, 64−71. (b) Smith, R. D.; Loo, J. A.; Edmonds, C. G.; Barinaga, C. J.; Udseth, H. R. *Anal. Chem.* **1990**, *62*, 882−899.

(15) Marquis-Rigault, A.; Dupont-Gervais, A.; Baxter, P. N. W.; Van Dorsellaer, A.; Lehn, J. M. *Inorg. Chem.* **1996**, *35*, 2307−2310. Hirsch, K. A.; Wilson, S. R.; Moore, J. M. *J. Am. Chem. Soc.* **1997**, *119*, 10401−10412 and references therein.

(16) Huck, W. T. S.; Hulst, R.; Timmerman, P.; van Vegel, F. C. J. M.; Reinhoudt, D. N. *Angew. Chem., Int. Ed. Engl.* **1997**, *36* (9), 1006−1008. (b) Moucheron, C.; Kirsch-De Mesmaeker, A. *J. Am. Chem. Soc.* **1996**, *118*, 12834−12835. (c) Kriesel, J. W.; König, S.; Freitas, M. A.; Marshall, A. G.; Leary, J. A.; Tilley, T. D. *J. Am. Chem. Soc.* **1998**, *120*, 12207−12215.

(17) McLafferty, F. W. *Science* **1981**, *214*, 280−287.

(18) (a) Biemann, K.; Martin, S. A. *Mass Spectrom. Rev.* **1987**, *6* (1), 1−76. (b) Biemann, K. *Pract. Spectrosc.* **1990**, *8 (Mass Spectrom. Biol. Mater.)*, 3−24. (c) Hines, W. M.; Falick, A. M.; Burlingame, A. L.; Gibson, B. W. *J. Am. Soc. Mass Spectrom.* **1991**, *3*, 326−336.

(19) (a) Somogyi, A.; Wysocki, V. H. *J. Am. Soc. Mass Spectrom.* **1994**, *5*, 704−717. (b) Downard, K. M.; Biemann, K. *J. Am. Soc. Mass Spectrom.* **1994**, *5*, 966−975.

(20) (a) Lias, S. G.; Liebmann, J. F.; Levin, R. D. *J. Phys. Chem. Ref. Data* **1984**, *13*, 695. (b) Smith, B. J.; Radom, L. *J. Am. Chem. Soc.* **1993**, *115*, 4885−4888. (c) Hillebrand, C.; Klessinger, M. *J. Phys. Chem.* **1996**, *100*, 9698−9702. (d) Szulejko, J. E.; McMahon, T. B. *J. Am. Chem. Soc.* **1993**, *115*, 7839−7848. (e) Meat-Ner, M.; Sieck, L. W. *J. Am. Chem. Soc.* **1991**, *113*, 4448−4460.

(21) Hummelen, J. C.; van Dongen, J. L. J.; Meijer, E. W. *Chem. Eur. J.* **1997**, *3* (9), 1489−1493.

(22) (a)Koper, G. J. M.; van Genderen, M. H. P.; Elissen-Roman, C.; Baars, M. W. P. L.; Meijer, E. W.; Borkovec, M. *J. Am. Chem. Soc.* **1997**, *119*, 6512−6521. (b) Kabanov, V. A.; Zezin, A. B.; Rogacheva, V. B.; Gulyaeva, Zh. G.; Zansochova, M. F.; Joosten, J. G. H.; Brackman, J. *Macromolecules* **1998**, *31*, 5242−5144.

(23) van Genderen, M. H. P.; Baars, M. W. P. L.; van Hest, J. C. M.; de Brabander-van den Berg, E. M. M.; Meijer, E. W. *Rec. Trav. Chim. Pays-Bas* **1994**, *113*, 573−574.

(24) Arnett, E. M.; Jones, F. M.; Henderson, W. G.; Beauchamp, J. L.; Holtz, D.; Taft, R. W. *J. Am. Chem. Soc.* **1972**, *94*, 4724−4726.

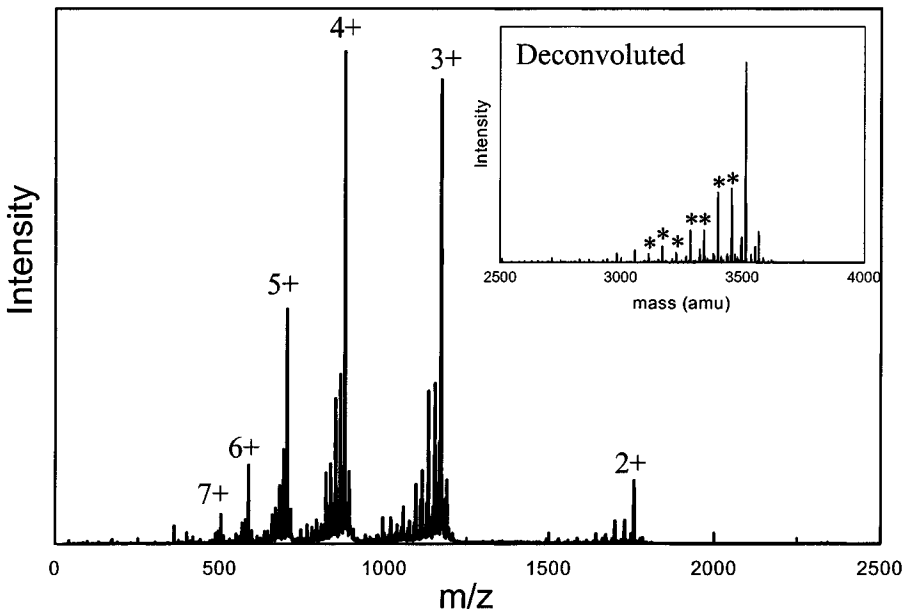

Figure 1. Single MS mode spectrum of DAB-*dendr*-$(NH_2)_{32}$. The asterisks indicate defects caused by missing Michael reactions.

ions of the poly(propylene imine) dendrimers of generation one through five, using MS^n. These gas-phase fragmentation patterns are subsequently compared with fragmentation that occurs upon prolonged heating in solution. These results show that mass spectrometry not only is very useful to characterize dendrimer structures but also provides detailed insight into the reactivity of these well-defined macromolecules.

Experimental Section

The poly(propylene imine) dendrimers (Astramol) were obtained from DSM (Geleen, The Netherlands). In this study both the amine- and the nitrile-terminated dendrimers were used up to the fifth generation. Measurements were performed on a Perkin-Elmer Sciex API 300 triple quad mass spectrometer (PE-Sciex, Foster City) with an *m*/*z* range of 3000. Nitrogen (N_2) was used as curtain gas and as CAD-gas in the collision cell. The triple quad MS is a tandem arrangement in which the first and third quads are mass selective and the second quad, operated in the rf only mode, serves as a collision cell. This arrangement is usually called a triple quadrupole (QqQ) and allows one to perform low-energy collisions (1−100 eV). In the MS^2 mode, the first mass filter Q1 filters the ions generated in the electrospray according to their mass-to-charge ratio. Ions of a specific *m*/*z* are selected and leave Q1 into the collision cell (q), where they are fragmented with neutral gas molecules (N_2) in a process referred to as collisionally activated dissociation (CAD). The resulting fragment ions pass into Q3 and are again filtered to provide a spectrum. The ions created by the source are generally referred to as precursor ions; the collision products are referred to as fragment ions. MS^3 is obtained by fragmenting the precursor ion with the curtain gas in the nozzle-to-skimmer interface, that is, in source fragmentation, followed by fragmentation in the collision cell.[25]

The dendrimer samples with a concentration of ~25 μM in MeOH/H_2O (75:25) were directly injected into the triple quadrupole mass spectrometer using a syringe pump (Harvard Apparatus, MA) at a flow rate of 5 μL/min. In the experiments used to determine the generation-dependent degree of the charging, a 10 mM ammonium acetate buffer (pH = 8.6) was used. Dry air was used as a nebulizer gas at a flow rate of 1.04 L min^{-1}. A voltage of 5.4 kV was applied to the capillary. In the single-MS and MS/MS mode, the orifice was typically set at 35 V, whereas in the MS^3 experiments various higher orifice values were used. Molecular modeling computational results were obtained using software programs from Molecular Simulations Inc. Force field calculations were carried out with the Discover program using the CVFF force field, and graphical displays were printed out from the Insight II molecular modeling system.

(25) Smith, R. D.; Loo, J. A.; Edmonds, C. G.; Barinaga, C. J.; Udseth, H. R. *Anal. Chem.* **1990**, *62*, 882−899.

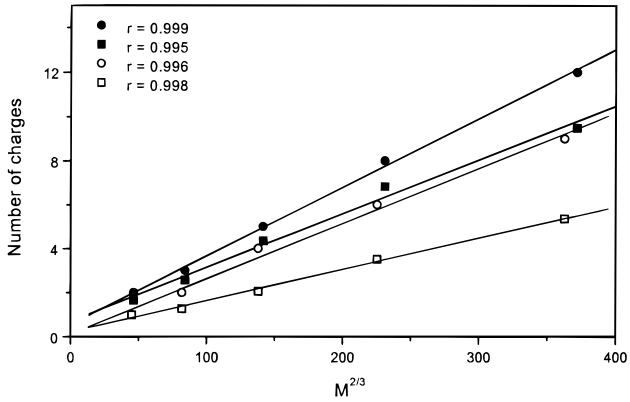

Figure 2. The average and maximum number of charges vs $M^{2/3}$ for amine and nitrile terminated dendrimers generations 1−5: (●) maximum number of charges for amine terminated dendrimers, (■) average number of charges for amine terminated dendrimers, (○) maximum number of charges for nitrile terminated dendrimer, (□) average number of charges for nitrile terminated dendrimers.

Results and Discussion

DAB-*dendr*-$(NH_2)_n$ and DAB-*dendr*-$(CN)_n$ (n = 4, 8, 16, 32, and 64) are polar and poly-basic compounds that are partially protonated, when dissolved in methanol−water mixtures. This property allows for the direct analysis of these solutions by positive ion ESI-MS. In a typical single MS mode spectrum of a poly(propylene imine) dendrimer, next to defect-free singly and multiply charged species, peaks assigned to defects in the dendrimers are present (Figure 1).

In Figure 2 both the average and the maximum number of charges are plotted against $M^{2/3}$ for amine- and nitrile-terminated dendrimers of generations 1−5.

As can be derived from Figure 2 a good linear relationship ($r > 0.99$) is obtained in all cases, consistent with the generally accepted spherical shape of these macromolecules in the gas phase.[26] Unlike linear polymers, exhibiting an almost linear relationship between charge capacity and molecular weight,[27] dendrimers are unable to extend their conformation completely

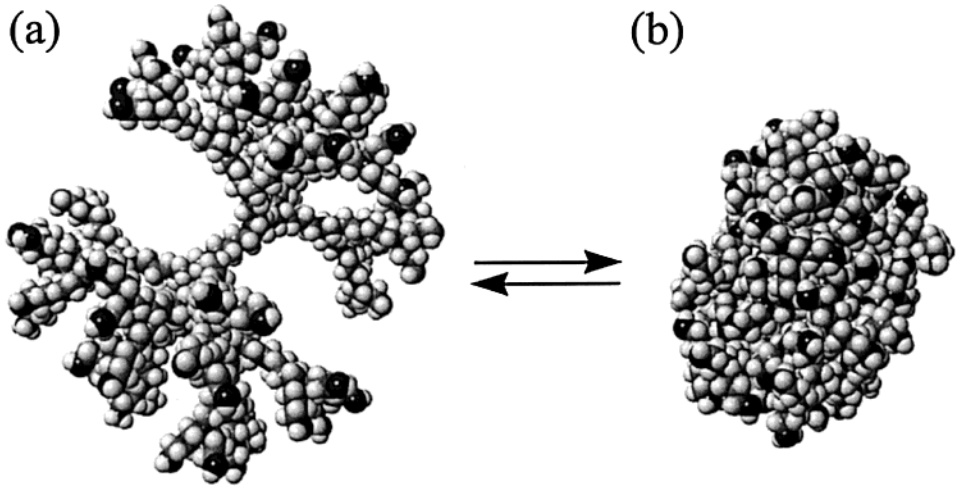

Figure 3. Gas-phase molecular modeling pictures of a fifth generation dendrimer (a) fully protonated, (b) Nonprotonated.

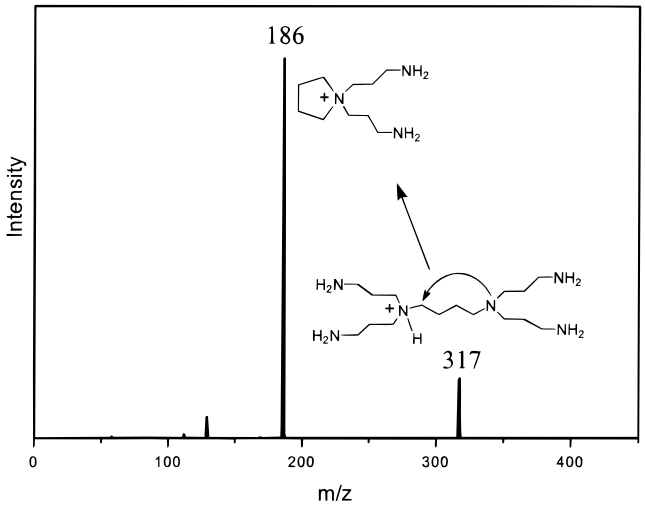

Figure 4. Formation of *m*/*z* 186 from $[M + H]^+$ of DAB-*dendr*-$(NH_2)_4$.

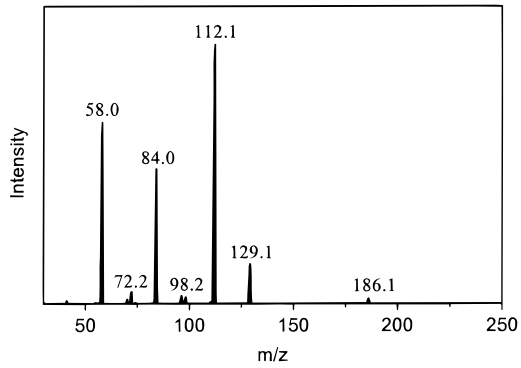

Figure 5. Fragmentation spectrum obtained from CAD on *m*/*z* 186.

upon charging. This feature results in a different charging behavior for dendrimers as compared to linear polymers.[26] The globular structure is also supported by gas-phase molecular modeling (Figure 3) obtained in case of a fully protonated fifth generation dendrimer (left) versus a nonprotonated dendrimer (right). Interatomic distances were calculated by a minimization of the free energy using the CVFF force field. In case of a nonprotonated dendrimer, a "dense core" structure is obtained due to intramolecular van der Waals forces. Protonation causes an expansion of the dendrimer and, hence, results in a change of the density profile. This ultimately leads to a "hollow core, dense shell" situation in case of a fully protonated dendrimer. These results indicate that, although the degree of protonation does affect the size of the dendrimers, their spherical nature in the gas phase is retained.

The study of the gas-phase fragmentations was initialized by performing Collision Activated Dissociation (CAD) on the $[M + H]^+$ ions of the first three generations. The fragmentation of $[M + H]^+$ from DAB-*dendr*-$(NH_2)_{32}$ (*m*/*z* 3515) and DAB-*dendr*-$(NH_2)_{64}$ (*m*/*z* 7169) was not feasible due to the limited *m*/*z* range (*m*/*z* range = 3000) of the ESI-MS apparatus. Subsequently, CAD was performed on multiply charged dendrimers. Precursor ion scans and gradient CAD (stepwise increase of the collisional energy) were used to unravel the fragmentation mechanisms. Generally, multiple collisions at low energy will increase the vibrational and excitation energies of the ions, giving rise to possible rearrangements before fragmentation. As a result mechanistic studies in the low-energy region are often speculative. However, the different generations of dendrimers studied here, both as single and as multiple charged species, show specific fragmentation patterns that prompt us to use an explanation in which the fragmentation pathways are governed by the initial site of protonation in case of singly charged dendrimers and by Coulomb repulsions in case of multiply charged dendrimers. In selected cases the defects present within the dendrimer were used as a label to monitor the fragmentation pathway. The characteristic gas-phase fragmentation patterns obtained in this way were subsequently compared with the fragmentation obtained after prolonged heating in solution.

Fragmentation of Singly Charged Dendrimers. The fragmentation of $[M + H]^+$ from DAB-*dendr*-$(NH_2)_4$ (*m*/*z* 317) was taken as a starting point, and the knowledge obtained from its fragmentation pattern was subsequently extrapolated to the higher generation dendrimers. CAD of $[M + H]^+$ led exclusively to the formation of *m*/*z* 186. This observation can only be accounted for by assuming that one of the diaminobutane (DAB) nitrogen atoms is protonated, while the other one acts as a nucleophile, leading to an intramolecular nucleophilic displacement reaction with subsequent loss of bis(propylamine) amine as illustrated in Figure 4.

CAD performed on *m*/*z* 186 led to the formation of *m*/*z* 169, 129, 112, 98, 84, 72, and 58 (Figure 5).

(26) (a) Schwartz, B. L.; Rockwood, A. L.; Smith, R. D. *Rapid Commun. Mass Spectrom.* **1995**, *9*, 1552−1555. (b) Tolic, L. P.; Anderson, G. A.; Smith, R. D.; Brothers, H. M.; Spindler, R.; Tomalia, D. A. *Int. J. Mass Spectrom. Ion Processes* **1997**, *165/166*, 405−418.

(27) Wong, S. F.; Meng, C. K.; Fenn, J. B. *J. Phys. Chem.* **1988**, *92*, 546−550.

Scheme 2. Formation of the Fragment Ions Resulting from CAD of *m*/*z* 186

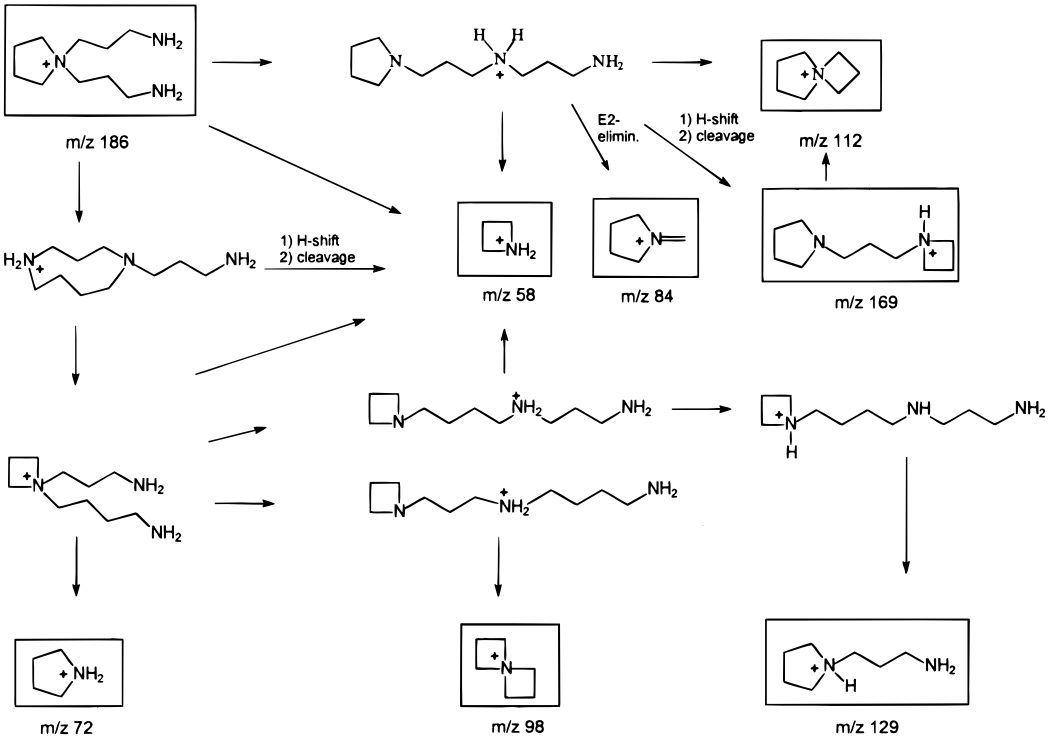

This characteristic fragmentation pattern can be explained completely when, next to nucleophilic displacement reactions, rearrangements and proton shifts are taken into account as depicted in Scheme 2. The reaction leading to *m*/*z* 84 most likely involves an intramolecular base-assisted E2 reaction.

It should be stressed here that, although the overview of reaction pathways outlined in Scheme 2 accounts for all of the signals observed, it is still incomplete. There are many other similar routes feasible leading to the fragments observed; these, according to our judgment, less favorable pathways have been omitted for clarity reasons. It is impossible to determine the extent to which each individual reaction pathway contributes to the formation of the particular fragment ions. Anyway, one would expect *m*/*z* 58 and 112 to be predominant, because there are many conceivable reaction pathways leading to these more stable fragments and this was indeed observed experimentally.

The main fragmentation pattern of $[M + H]^+$ for DAB-*dendr*-$(NH_2)_8$ (*m*/*z* 774) and DAB-*dendr*-$(NH_2)_{16}$ (*m*/*z* 1687) is essentially the same and involves a cascade reaction as is shown in Figure 6 for DAB-*dendr*-$(NH_2)_{16}$. The first step consists of a cleavage of the central DAB core, analogous to DAB-*dendr*-$(NH_2)_4$, leading to a cleaved dendrimer carrying a charged five-membered heterocyclic ring, which acts as the leaving group in the second nucleophilic displacement reaction along the cascade. The charged four-membered ring formed during this process subsequently acts as the leaving group in the third nucleophilic displacement reaction. Hence, during each nucleophilic displacement reaction, the leaving group for the next displacement along the chain is introduced.

As anticipated, CAD performed on the separate ions in the chain led to the formation of the subsequent fragment ions along the chain. The cascade of nucleophilic displacement reactions is terminated by the formation of the azetidinium ion *m*/*z* 58 from *m*/*z* 172, which cannot fragment any further. However, CAD of *m*/*z* 172 also yields *m*/*z* 155, 115, and 98 next to *m*/*z* 58. The proposed formation of these fragment ions from *m*/*z* 172 is outlined in Scheme 3.

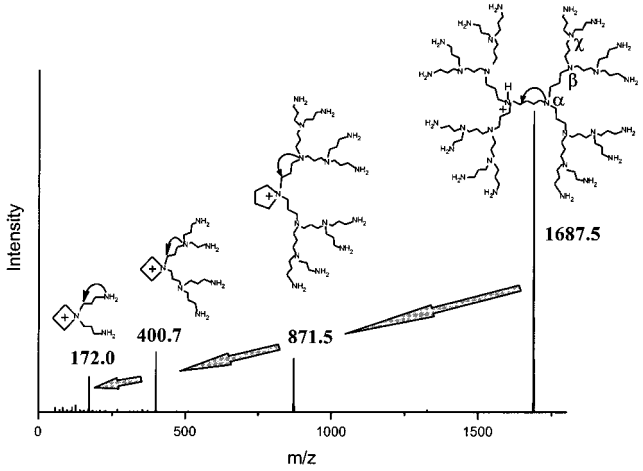

Figure 6. Main fragmentation pattern for $[M + H]^+$ from DAB-*dendr*-$(NH_2)_{16}$.

There is a striking resemblance between Schemes 2 and 3. Scheme 2 involves pyrrolidinium dissociation, whereas Scheme 3 describes azetidinium dissociation. Comparison of the two shows that precursor ions and fragment ions in both schemes are related through $\Delta m/z = 14$ (four- vs five-membered ring) and that the same mechanistic pathways are involved.

Alternatively, all of the fragments depicted in Figure 6 can also be envisaged as directly resulting from $[M + H]^+$. In that case the protonation site determines which particular fragment ion is formed. Protonation of the β-nitrogen atom, for instance, could give rise to the direct formation of *m*/*z* 172, whereas dendritic ions carrying a γ-protonated nitrogen atom could directly yield *m*/*z* 58. It is obvious that the gas-phase basicity of the tertiary nitrogen atoms in the successive dendritic layers determine the extent to which both mechanisms are operative.

To investigate the site of protonation in $[M + H]^+$ from DAB-*dendr*-$(NH_2)_n$ ($n = 4, 8, 16$), we performed very mild CAD on the $[M + H]^+$ ions, limiting successive fragmentations to a

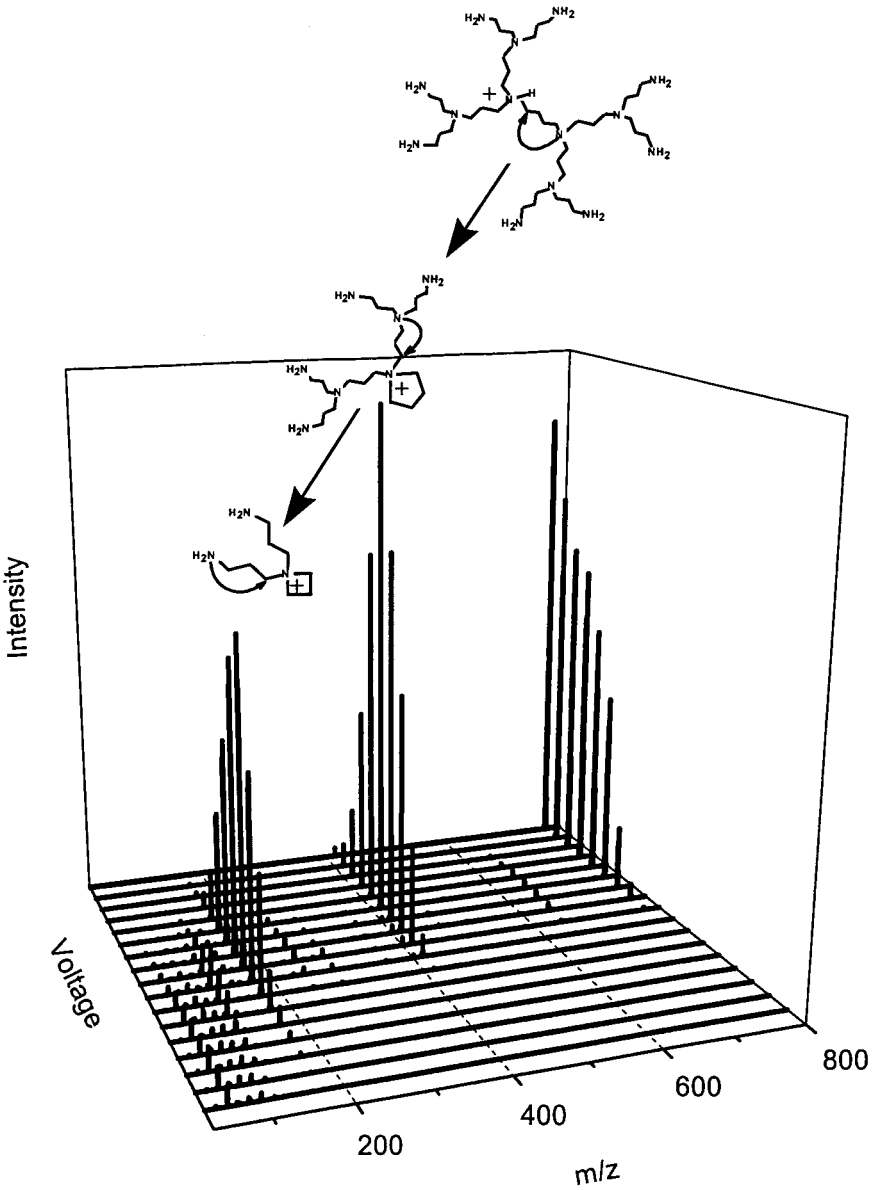

Figure 7. Effect of increasing the collisional energy on the fragmentation of $[M + H]^+$ from DAB-*dendr*-$(NH_2)_8$.

Scheme 3. Formation of the Fragment Ions Resulting from CAD of *m*/*z* 172

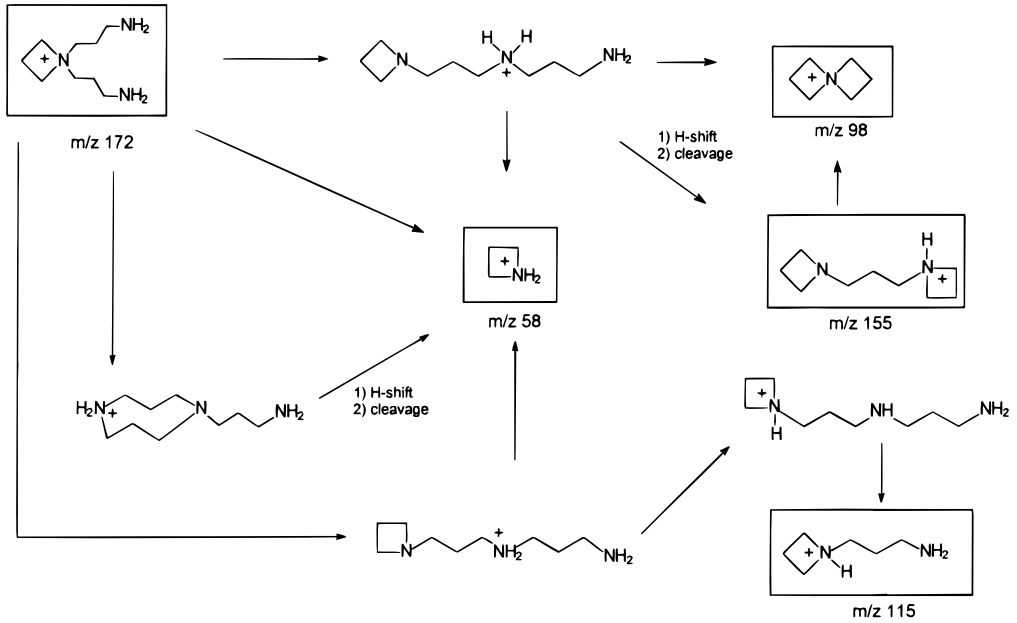

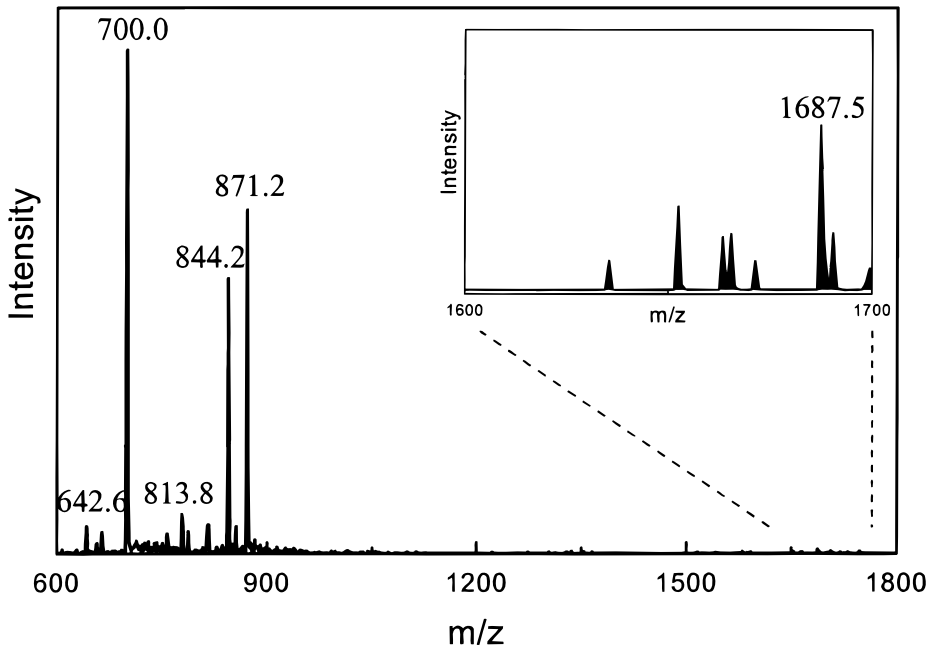

Figure 8. Precursor ion scan on *m*/*z* 400 derived from fragmentation of DAB-*dendr*-$(NH_2)_{16}$.

Scheme 4. Interpretation of Precursor Ion Scan of *m*/*z* 400 from DAB-*dendr*-$(NH_2)_{16}$

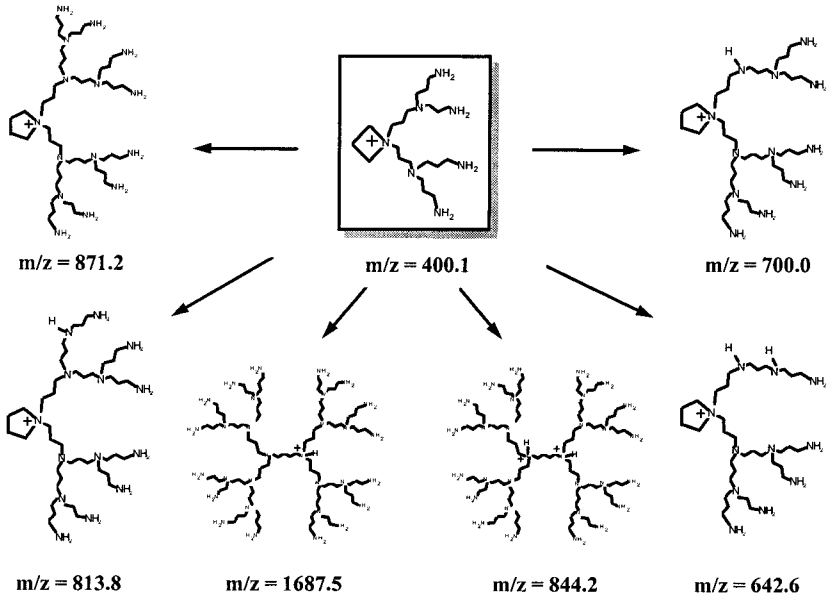

negligible extent. The fragments thus obtained provide information regarding the initial position of the proton in the precursor ion. In all cases, mild fragmentation led predominantly to the formation of central core cleaved dendrimers, indicating that the tertiary DAB nitrogen atoms are the most basic ones in all three generations. The effect of increasing the fragmentation energy is depicted in Figure 7. At very low voltages, splitting of the dendrimer core is observed. Stepwise increase of the voltage, and hence of the collisional energy, allows for the subsequent dissociation along the chain to occur. Accordingly, the cascade mechanism is the main mechanism operative, although the direct formation of the chain fragments from $[M + H]^+$ does occur to a slight extent as well.

Unambiguous proof of the cascade fragmentation mechanism was obtained by performing precursor ion scans on the separate ions in the chain. A typical example of a precursor ion scan is shown in Figure 8 for *m*/*z* 400 from DAB-*dendr*-$(NH_2)_{16}$.

The information obtained from this particular precursor ion scan is shown in Scheme 4. Evidently, *m*/*z* 400 is derived not only from the half dendrimer at *m*/*z* 871 but also from half dendrimers exhibiting a defect and to a negligible extent directly from $[M + H]^+$ and $[M + 2H]^{2+}$.

The desolvation process during which ions in solution are converted to ions in the gas phase requires different energies of activation for different ions. This implies that the relative intensities of peaks in the mass spectra obtained cannot be used as a measure for their relative abundances in solution. A different situation arises when intramolecular gas-phase reactions are involved; in this case both precursor ions and fragment ions have the same response factors and hence their relative intensities can directly be compared. This is nicely illustrated in the fragmentation of defect-containing dendrimers. A defect present in the dendrimer can be used as a label that will be statistically distributed over the fragment ions, as is shown in Figure 9 for a defect DAB-*dendr*-$(NH_2)_{16}$ missing one propylamine unit.

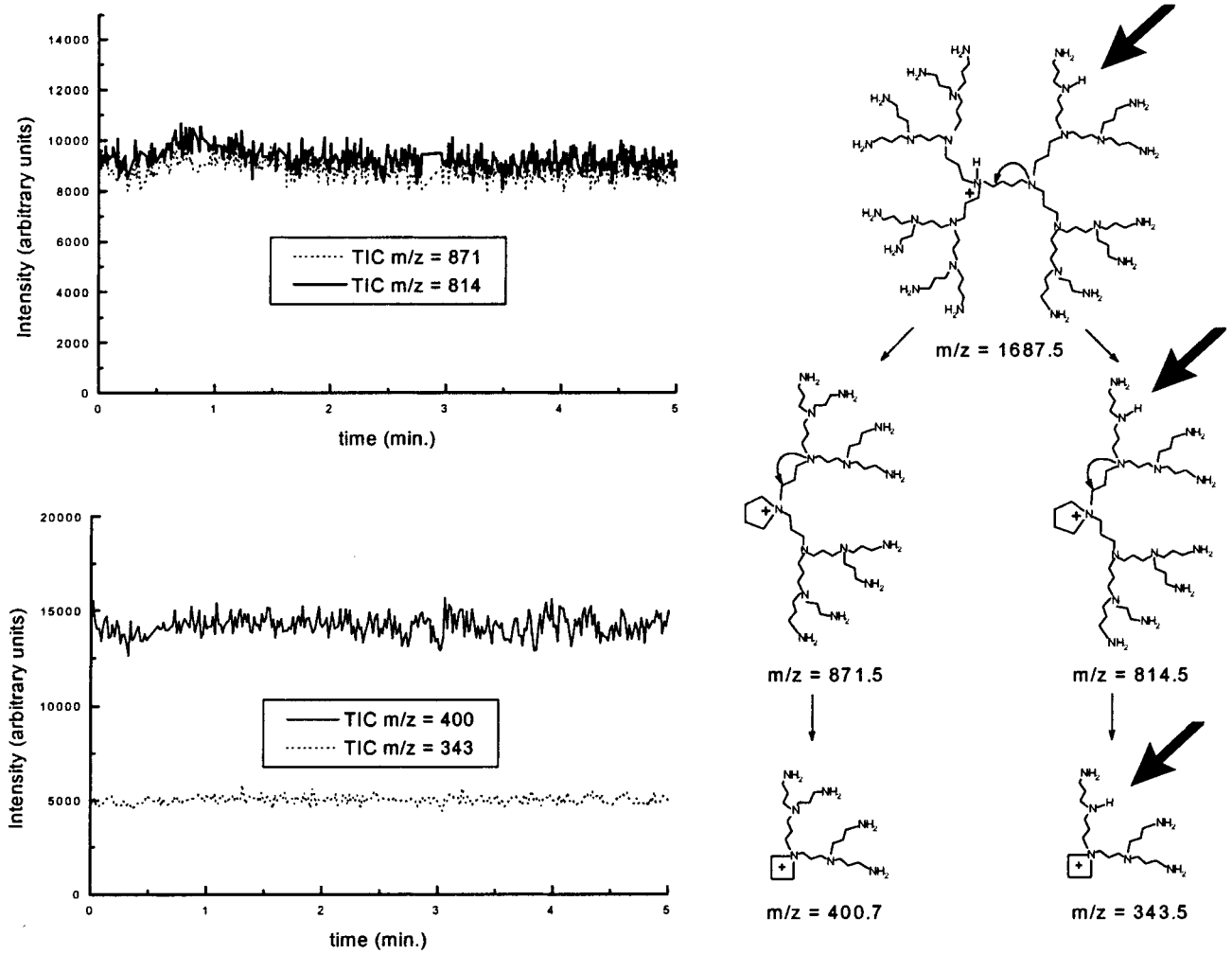

Figure 9. TIC spectra showing equal gas-phase response for the fragments ions derived from a defect DAB-*dendr*-$(NH_2)_{16}$.

Each fragment ion that is generated induces a small electrical current. In this way the total ion current (TIC) generated for each fragment ion provides a measure for its relative intensity. As can be derived from Figure 9, dissociation of $[M - 57 + H]^+$ yields two split dendrimers in a 1:1 ratio: a perfect "half" dendrimer at *m*/*z* 872 and a defect one at *m*/*z* 815. Subsequent fragmentation of these core-split dendrimers yields *m*/*z* 400 and *m*/*z* 400−57 in a 3:1 ratio, as expected. These results implicate that the relative fragment ion intensities reflect the significance of the reaction that led to their formation.

Fragmentation of Multiply Charged Dendrimers. In the case of DAB-*dendr*-$(NH_2)_4$, the fragmentation of $[M + 2H]^{2+}$ (*m*/*z* 159) did not show the characteristic splitting of the dendritic core as was the case for the $[M + H]^+$ ion. Instead, fragment ions were observed at *m*/*z* 150, 142, 260, 129, and 58. The first two ions in this row are doubly charged and are formed through the loss of one or two neutral NH_3 molecules from the precursor ion, respectively. Hence, the ions at *m*/*z* 150 and 142 suggest a precursor ion carrying two protonated primary amines in the outer shell. The ions at *m*/*z* 260, 129, and 58 are all singly charged and are fragment ions resulting from $[M + 2H]^{2+}$ ions carrying one protonated primary amine and one protonated tertiary amine. The ion at *m*/*z* 260 can be viewed as a defect dendrimer missing one propylamine unit and, therefore, contains three different types of amines: one tertiary, one secondary, and three primary ones. Since there is only one proton present this will probably be located at the most basic site in the molecule, which is the tertiary amine in the core. Fragmentation of this ion most likely involves a nucleophilic displacement reaction in which the DAB core is cleaved and the *m*/*z* 129 ion is formed. In a control experiment, the same fragmentation pattern was observed for a "real" defect dendrimer, missing one propylamine unit. Dendrimers with a fully protonated diaminobuthane core and dendrimers carrying three or more charges were not observed due to the unfavorable Coulomb repulsions associated with these ions.

In the case of DAB-*dendr*-$(NH_2)_8$, multiply charged ions carrying 2 or 3 protons were observed. Neither of these ions showed a cleavage of the central DAB core upon CAD; therefore the chain mechanism, characteristic for the $[M + H]^+$ ions, was absent from the fragmentation spectrum of the multiply charged ions. Fragment ions were indicative of the presence of charge on the β- and γ-nitrogen atoms. Only in the case of $[M + 2H]^{2+}$, one of the α-nitrogen atoms was protonated. This led to the formation of 1,1-bis(propylamine)azetidinium (*m*/*z* 172) and a "defect" dendrimer missing one wedge at *m*/*z* 603. Analogous to the fragmentation of *m*/*z* 260 described above, subsequent splitting of the dendritic core led to the formation of a core-cleaved dendrimer missing one wedge at *m*/*z* 243.

The fragmentation pattern of the third generation dendrimer forms an intermediate case between the first and the second generation on one hand and the fourth and fifth generation on the other. The fragmentation behavior of the $[M + 2H]^{2+}$ resembles that of the previous generations, whereas the fragmentation pattern for $[M + 3H]^{3+}$ and $[M + 4H]^{4+}$ is analogous to that observed for higher generations. CAD performed on [M

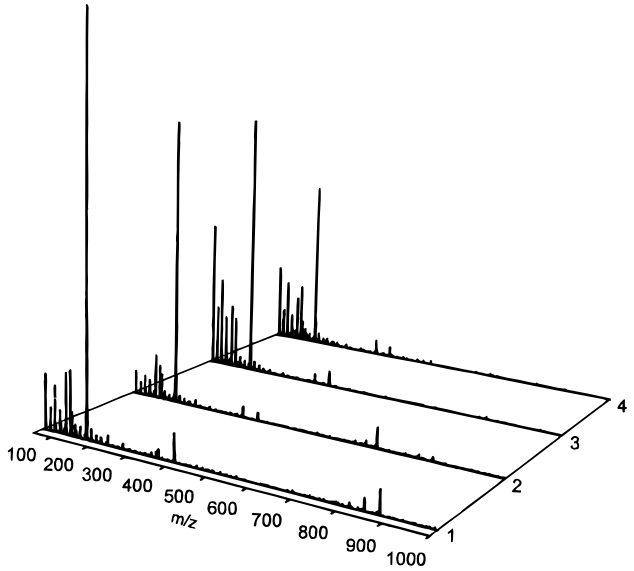

Figure 10. Formation of $m/z = 172$ and fragments derived thereof in case of (1) [DAB-*dendr*-$(NH_2)_{32}$ + 4H]$^{4+}$, (2) [DAB-*dendr*-$(NH_2)_{32}$ + 5H]$^{5+}$, (3) [DAB-*dendr*-$(NH_2)_{64}$ + 5H]$^{5+}$, and (4) [DAB-*dendr*-$(NH_2)_{64}$ + 6H]$^{6+}$.

+ 2H]$^{2+}$ was again indicative of charges located in the outer dendritic layers, whereas the fragmentation of [M + 3H]$^{3+}$ and [M + 4H]$^{4+}$ yielded predominantly *m*/*z* 172 and fragments derived thereof. The rationale behind the predominant formation of bis(propylamine) azetidinium (*m*/*z* 172) in the latter cases will be presented below.

For DAB-*dendr*-$(NH_2)_{32}$ and DAB-*dendr*-$(NH_2)_{64}$, charge clusters appeared between 2−8 and 5−12, respectively. In all cases low-energy CAD yielded predominantly *m*/*z* 172 and fragments derived thereof as illustrated in Figure 10. Although the predominant formation of the *m*/*z* 172 fragment can in principle be the result of high-energy collisions, the experimental conditions of 1−100 eV used here are generally accepted to be low enough to exclude high-energy fragmentations.

From this point of view, the almost exclusive formation of *m*/*z* 172 is a surprising result, because a fifth generation dendrimer contains 62 tertiary amines over which the available protons can be spread, and when proton shifts and rearrangements are taken into account, a large number of product ions can be expected. However, judging from Figure 10, it seems obvious that electrostatic interactions play a predominant role in the fragmentation process of the higher generations multiply charged dendrimers. Due to the spherical shape of the dendrimer, over which the charges are probably evenly distributed,[28] three different kinds of nucleophilic displacement reactions can be recognized from an electrostatic point of view (Figure 11). The nucleophilic displacement reactions depicted in Figure 11 are proposed to be increasingly favored on going from top to bottom.

The nucleophilic displacement reaction of type A involves an ϵ-shell-protonated nitrogen atom and a δ-shell nucleophile. During the inside-to-outside nucleophilic attack, a neutral leaving group (bis(propylamine)amine) is lost. In this reaction the positive charge moves inward and gets in closer proximity to the other charges present in the molecule, which is an unfavorable process. The second type of nucleophilic displacement reaction (B) also involves an ϵ-shell-protonated nitrogen atom, but in this case, a neighboring ϵ-shell nitrogen atom acts as a nucleophile in the displacement of the neutral leaving group. Hence, in this case the positive charge does not move inward but resides in the same shell. The last type (C) of nucleophilic displacement reaction involves an outside-to-inside nucleophilic attack giving rise to the formation of *m*/*z* 172. This third case is more favorable than the previous two because it involves a charged leaving group leading to a splitting of positive charges during the nucleophilic displacement reaction.

Fragmentation of Dendrimers in Solution. The fragmentation of all generations of poly(propylene imine) dendrimers was studied in pure methanol and in methanol/water mixtures (3:1) at 70 °C. Dendrimers dissolved in pure methanol were stable for weeks at 70 °C. In methanol/water (3:1) mixtures, the first two generations of dendrimer were stable for more than 2 weeks, whereas generations 3−5 showed fragmentation after 6 days under the same conditions. The decrease in stability upon addition of water is due to the higher degree of protonation of the dendrimer. Upon addition of a small amount of acetic acid to a fifth generation dendrimer, decomposition was observed within 1 h at 70 °C.

Special attention was paid to the fragments obtained in the $m/z < 180$ region for which a striking similarity with the gas-phase fragmentation adducts was found, as is shown in Figure 12 for DAB-*dendr*-$(NH_2)_{16}$. The small differences are attributed to the fact that, in solution next to the [M + 3H]$^{3+}$ ions, also other multiply charged species and defect dendrimers are present.

For DAB-*dendr*-$(NH_2)_{32}$ and DAB-*dendr*-$(NH_2)_{64}$ a perfect match for $m/z < 180$ was obtained similar to the one presented in Figure 12 for DAB-*dendr*-$(NH_2)_{16}$. At $m/z > 180$, a remarkable difference arises with the gas-phase fragmentation from the observation of *m*/*z* 360, which is attributed to γ- and δ-shell-protonated dendrimers, respectively.

In case of DAB-*dendr*-$(NH_2)_{64}$, the formations of *m*/*z* 360 and *m*/*z* 172 both involve a δ-shell-protonated dendrimer. As explained earlier with Figure 11, the outside-to-inside nucleophilic attack by an ϵ-shell nitrogen atom is favored in the gas phase and yields *m*/*z* 172. The ion at *m*/*z* 360 is proposed to arise from a δ-shell-protonated dendrimer that is attacked by a γ-shell nitrogen nucleophile via an inside-to-outside attack. The formation of *m*/*z* 360 in the gas phase is very unfavorable from an electrostatic point of view, since it involves a nucleophilic displacement reaction in which a large neutral dendritic wedge is lost, leaving a smaller dendrimer behind carrying the same number of charges. The observation of this ion in solution illustrates that Coulomb repulsions are less important in solution as compared to the gas phase due to solvent interactions; although less important they cannot be ignored judging from the formation of *m*/*z* 172.

Conclusions

The charging behavior of the poly(propylene imine) dendrimers, as studied here by positive ion ESI-MS, confirms the generally accepted idea of an on-the-average spherical shape for these molecules in the gas phase. Unique fragmentation patterns are observed, due to the globular shape of the dendrimer. Fragmentation patterns of poly(propylene imine) dendrimers generations 1−5 can be explained when, next to nucleophilic displacement reactions, proton shifts and rearrangements are taken into account. Although it is generally accepted that low-energy collisions can lead to rearrangements prior to fragmentation, the dendritic fragments observed in this study prompts us to propose that the site of protonation within

(28) For a theoretical study involving the distribution of charges over a sperical surface see: Mahoney, J. F.; Kalensher, B. E.; Perel, J.; Lee, T. D. *Int. J. Mass Spectrom. Ion Processes* **1988**, *83*, 231−244.

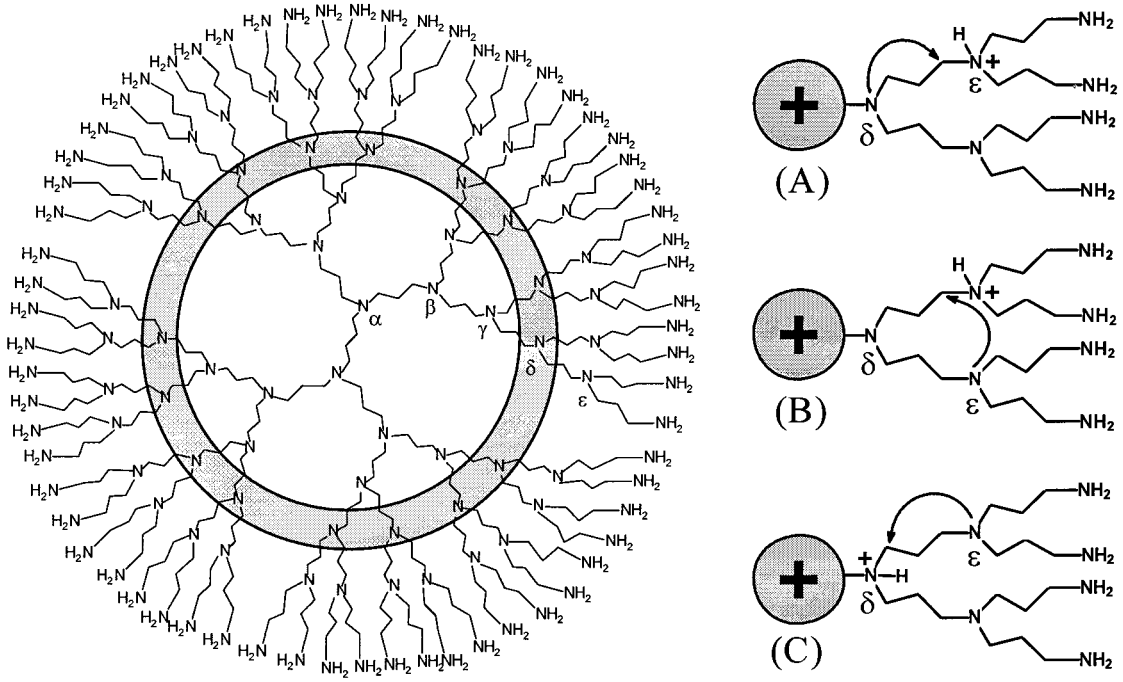

Figure 11. Classification of nucleophilic displacement reactions in three main types on the basis of electrostatic interactions.

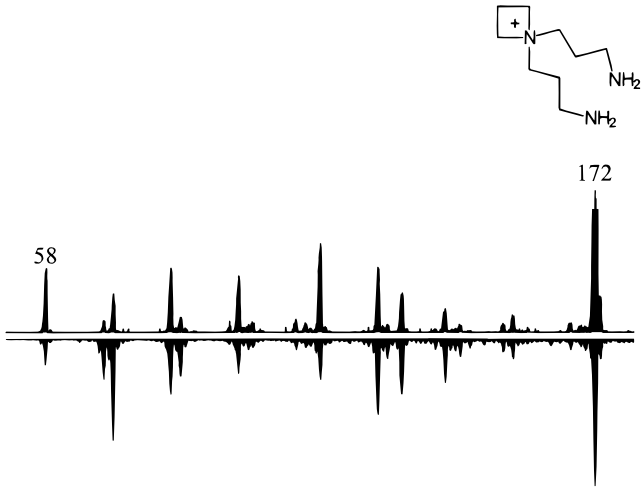

Figure 12. Fragmentation of DAB-*dendr*-$(NH_2)_{16}$: top, gas-phase fragmentation of $[M + 3H]^{3+}$ vs bottom, fragmentation in solution (10 days, $MeOH/H_2O$, 70 °C).

the dendrimer has a large impact on the fragmentation pathway and is largely dependent on both the relative proton affinities and the Coulomb repulsions between neighboring protonated sites. Dendrimers are ideal models to study these general phenomena in detail.

The fragmentation of the $[M + H]^+$ ions from DAB-*dendr*-$(NH_2)_n$ ($n = 4, 8, 16$) all follow the same mechanistic pathway involving a chain mechanism. This mechanism is the main one operative that can be understood in terms of the basicity of the nitrogen atoms in the successive dendritic layers. Apparently, the diaminobuthane (DAB) nitrogen atoms are the most basic ones present (in the gas phase), and hence, protonation almost exclusively leads to dendrimers carrying a protonated DAB core. Consequently, the first nucleophilic displacement reaction leads predominantly to a splitting of the dendrimer core, thus providing the initiator for a cascade of nucleophilic displacement reactions.

In the fragmentation of higher generation, multiply charged dendrimers electrostatic interactions play a predominant role. This eventually yields almost exclusively bis(1,1-propylamine)-azetidinium (*m*/*z* 172) and fragments derived thereof.

Finally, the fragmentation of dendrimers after prolonged heating in solution was investigated. The gas-phase fragmentations provided us with a very characteristic fingerprint of dendrimer degradation products in the lower *m*/*z* range (*m*/*z* < 180), which matched to a very high degree with the situation in solution. However, in case of the fourth and fifth generation dendrimers, a significant amount of *m*/*z* 360 was formed in solution, whereas this ion was not be observed in the corresponding gas-phase fragmentations. The appearance of this ion in solution illustrates that the role of electrostatic interactions is less prominent in solution as compared to the gas phase and is a result of solvent interactions. The results presented here show the power of electrospray mass spectrometry to study the reactivity of well-defined synthetic macromolecules.

Acknowledgment. The authors wish to thank M. Muré-Mak and E. M. M. de Brabander van den Berg for providing us with the poly(propylene imine) dendrimers. We are grateful to B. Coussens (DSM) for the molecular modeling calculations. DSM Research is gratefully acknowledged for an unrestricted research grant.

Supporting Information Available: Additional data on precursor ion scans, MS^3 experiments, and fragmentations of dendrimers in solution. This material is available free of charge via the Internet at http://pubs.acs.org.

JA984432+